Fracture Mechanics of Concrete and Concrete Structures -
High Performance, Fiber Reinforced Concrete, Special Loadings and Structural Applications- B. H. Oh, et al. (eds)

Experimental and numerical study towards a deformation-based seismic assessment of substandard exterior R.C. beam-column joints

G. Genesio & R. Eligehausen
University of Stuttgart, Stuttgart, Germany

A. Sharma
Bhabha Atomic Research Centre, Mumbai, India

S. Pampanin
University of Canterbury, Christchurch, New Zealand

ABSTRACT: In reinforced concrete framed structures under seismic excitations the beam-column joint cores are arguably one of the most vulnerable zone. Experimental tests have shown that the structural behavior of poorly detailed joints is decisive for the structural response of older frame buildings. Due to inadequate shear reinforcement in the joint, poor bond properties of longitudinal reinforcement and deficiencies in the anchorage of reinforcement, a brittle failure mechanism can be expected. In the numerical analysis of r.c. moment resisting frames the joint core is usually considered as rigid and all the plastic rotations are assumed to take place in the beams and/or columns. Although this assumption is reasonable for structures subjected mainly to gravity loads, it may be highly misleading for structures subjected to seismic loads. In the literature several methods to assess the shear resistance of beam-column connections were proposed, but the deformation capacity of joints was not deeply investigated yet. In this study exterior beam-column joints designed for gravity only (or mainly) loads as typical of old code provisions are considered. Experimental investigations were conducted in the laboratory of the Bhabha Atomic Research Centre (BARC) in Mumbai. Three exterior beam-column joints characterized by lack of shear reinforcement in the joint panel and by different anchorage solutions commonly used in the construction practice until the beginning of the 1970s were tested. Numerical analyses were carried out with the finite element (FE) Code MASA, developed at the University of Stuttgart and capable of three-dimensional (3D) nonlinear analysis of quasi-brittle materials, like concrete, based on the microplane material model. In both experimental and numerical investigations particular attention was given to the evaluation of the deformation capacity of the joint. The capability to numerically reproduce the joint behavior was discussed and the influence of several parameters such as bond of longitudinal reinforcement of beam and column and shape of the anchored bars were investigated. The results were compared with the available data described in the literature and found in the tests.

1 INTRODUCTION

In many reinforced concrete structures, built all over the world in seismic-prone countries before the introduction of modern seismic oriented codes in the 1970s, the detailing of beam-column connection presents deficiencies such as: lack of joint hoops, use of plain round bars and poor anchorage of the beam bars in the core. These deficiencies may lead to a brittle failure of the connection and consequently of the whole frame. For this reason in many cases a seismic retrofit is urgently required. The first step of a retrofit strategy is the assessment of the capacity of the existing structural element in order to quantify its performance and the need of upgrade in terms of strength and ductility.

In this study, experimental tests on exterior beam-column joints detailed according to different construction practices, adopted before the introduction of modern seismic codes, were performed in the laboratory of BARC in Mumbai, India. Furthermore, numerical simulations were carried out with the finite element code MASA, developed at the University of Stuttgart and capable of 3D nonlinear analysis of concrete-like materials and reinforced concrete structures. The program is based on the microplane model with relaxed kinematic constraint (Ožbolt et al. 2001). Following a brief description of the investigated test specimens, the main features of the employed FE model are presented. The numerical analyses are compared with the experimental results.

In the present contribution particular emphasis is given to the joint shear behavior in terms of peak load, cracking pattern and core deformability. In this context a very important role is played by the formation of the first shear crack in the joint, since from that point the shear distortion start increasing.

Following a critical discussion about the failure mode observed in the experiments and numerical investigations, the influence of different parameter on the shear failure of the joint core was investigated.

2 JOINT ASSESSMENT METHOD

In this research work only the concrete contribution to the joint shear strength is taken into account. In most of the existing codes which consider the assessment of the joint shear capacity, the concrete stresses in the joint panel are limited by $(f_c')^{0.5}$ multiplied by a factor k_1 considering the failure of the tensile tie (ACI 318-05 and EC8) or limiting by $k_2 f_c'$ for the compressive strut failure (NZS 3101).

Also other assessment methods were proposed in the literature. In most of the cases the joint shear capacity considering only the concrete contribution is estimated as function of the squared root of concrete compressive strength. Furthermore, the influence of several parameter such as the joint aspect ratio (Vollum & Newman 1999) or additionally also the reinforcement ratio in the column (Hegger et al. 2002) is considered in different assessment models. In most of the existing models the anchorage of the beam bars in the core plays a secondary role.

Priestley (1997) proposed a formulation of the joint shear capacity in terms of principle tensile stress (p_t) calculated according to the Mohr's circle theory, taking into account also the effect of axial load in the column which deeply influences the joint shear capacity, as also confirmed by several experimental studies in the following literature, e.g. Pampanin et al. (2002). According to this formulation the limit for the principle tensile stress is given by $k(f_c')^{0.5}$, where k is a factor depending from the joint type (X-Joint, T-Joint or L-Joint) and in the case of T-Joint depending from the anchorage of the beam bars in the core (0.42 bent into the joint and 0.29 bent away from the joint) (Fig. 1a). Furthermore, Priestley (1997) proposed also limits for the joint deformability based on the available experience (Fig. 1b). Pampanin et al. (2002) investigated the case of plain round bars with 180° hooks and further developed the assessment model for existing beam column joints based on the evaluation of hierarchy of strength and sequence of events (Pampanin, 2006).

In this study the assessment method originally proposed by Priestley (1997) is considered, since it was shown that it is the most reliable for the case of substandard exterior beam-column joints (Hertanto 2006). A parametric study with the FE method is necessary in order to evaluate the influence of other parameters such as beam and column reinforcement ratio and joint aspect ratio, which are not taken into account in the existing model.

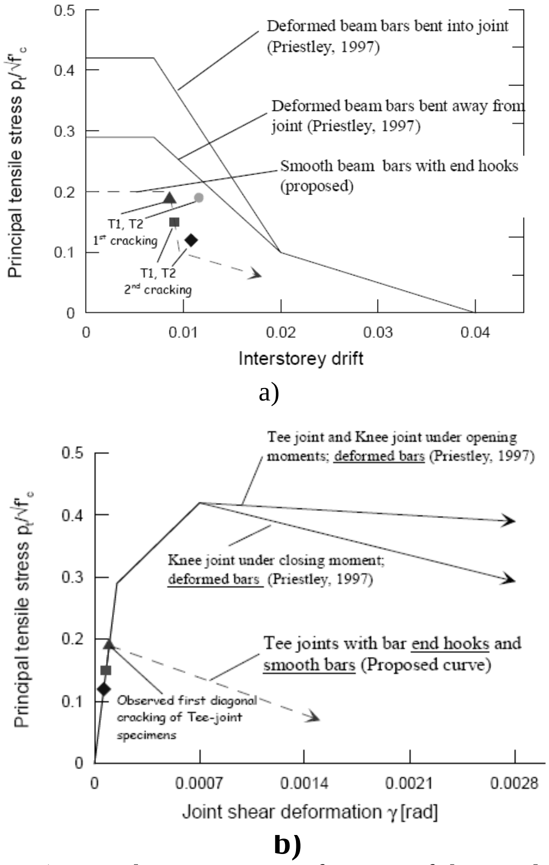

Figure 1. a) Joint shear capacity as function of the top drift; b) Joint shear capacity as function of the joint shear deformation (Priestley (1997), Pampanin et al. (2002)).

3 EXPERIMENTAL PROGRAM AND GENERAL RESULTS

In this research project three full scale exterior beam-column joints with the same geometry and different detailing of the anchorage of beam deformed bars in the joint were tested in the laboratory of the BARC (Fig. 2). The main aim of the experimental program was to investigate the influence of beam bar anchorages in the joint according to different non-seismic construction practices (Fig. 3). In the first test (JT1-1) the 90° bending into the joint according ACI 318-71 was chosen. The JT3-1 specimen was characterized by 150 mm straight anchorage of the bottom bars and in the JT4-1 specimen those bars were anchored with 90° hooks according to common East-Asiatic construction practice (Kurose 1987). All the specimens were designed to fail in shear in the joint panel, before the yielding of the beam bars occurred. The material properties of the specimens are summarized in Table 1.

The specimens were loaded cyclically at the beam end, while the column's top and bottom were hinged. The imposed loading history consisted of a series of two cycles at increasing displacement levels: ± 5, ± 10, ± 20, ± 30, ± 40, ± 60, ± 70 mm.

The application of a constant axial load can lead to unconservative results, because in the case of lateral loading of a moment resisting frame the asymmetric cyclic push-pull would induce a variation of the axial load, which could modify significantly the hierarchy of strength within a beam-column joint subassembly, as explained in Pampanin et al. (2002) and Pampanin (2006). Since this solution was not applicable with the available test setup, no axial load was applied on the column. This solution could arguably allow to obtain a conservative estimation of the joint shear capacity, although not capturing interaction effects due to the premature buckling of the column longitudinal bars.

During the tests the hysteretic behavior of the specimen as well the deformation contribution of beam, column and joint were measured. An overview of the results are herein summarized, while the detailed results of the test JT4-1 are presented in Section 5.1 in the comparison with the numerical simulations.

Table 1. Material properties of the test specimens.

Test Specimen		JT1-1	JT3-1	JT4-1
Steel	Bar [mm]	D8	D16	D20
	f_y [MPa]	548	558	552
	f_u [MPa]	652	688	672
	E_s [GPa]	200		
Concrete	f_c'[MPa]	25.4	27.5	28.2
	E_c [GPa]	28.5		

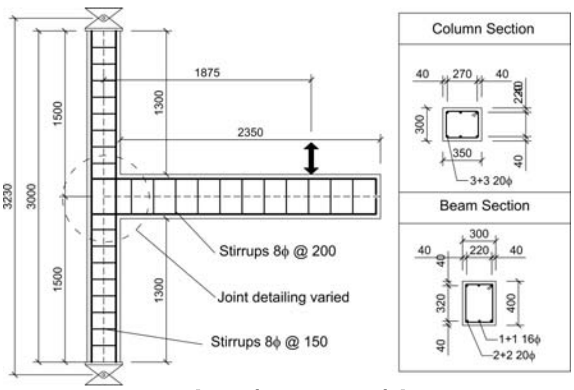

Figure 2. Geometry and reinforcement of the test specimens.

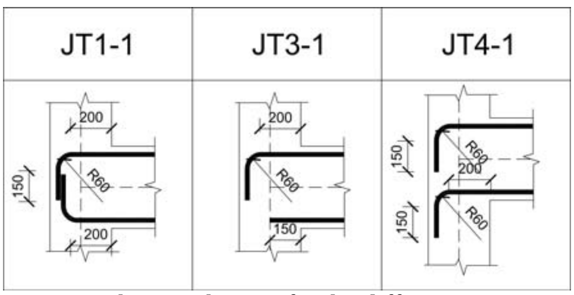

Figure 3. Beam bars anchorage for the different specimens.

As per design all the tested beam-column connections failed through shear cracking in the joint core, without any yielding of beam and column rebars.

In Figure 4 the envelopes of the lateral load-displacement curves obtained in the tests are presented. The final cracking patterns are shown in Figure 5. The specimen JT1-1 presented a symmetric diagonal cracking (Fig. 5a). In the specimen JT3-1, a reduced capacity was obtained under positive loading direction, due to the straight anchorage with no mechanical hook of the bottom bar and the shear crack started approximately at the end of the beam bar (Fig. 5b). Also in the specimen JT4-1 a reduced shear capacity in the positive loading direction was observed. This was due to the anchorage with 90° bending away from the core. The shear crack starting from the bottom bars is characterized by a lower angle against the horizontal axis (Fig. 5c). Similar observation for the case of bars bent away from the joint are also available in tests results in the literature (e.g. Kurose 1987).

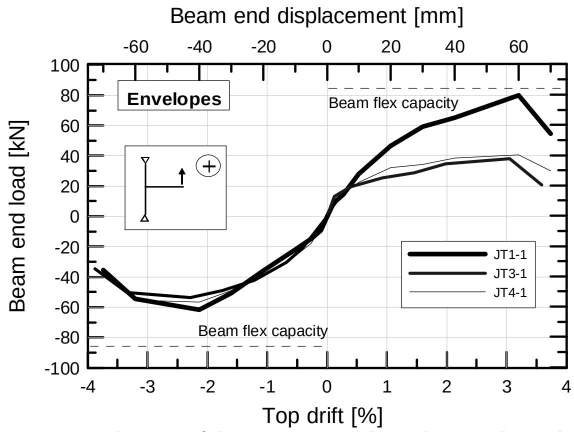

Figure 4. Envelopes of hysteretic cycles observed in the experimental tests.

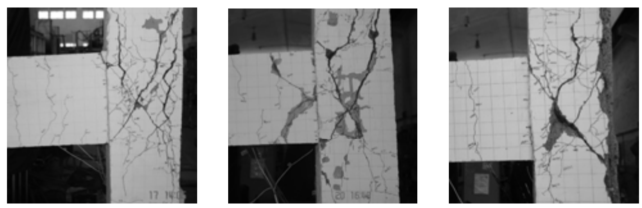

a) b) c)

Figure 5. Cracking pattern at end of the tests: a) JT1-1; b) JT3-1; c) JT4-1.

4 FINITE ELEMENT MODEL

In the FE Code used in the analysis, the microplane material model for concrete and 1D three-linear constitutive law for reinforcement steel were used.

The microplane model is a 3D macroscopic model in which the material is characterized by uniaxial relations between the stress and strain components on planes of various orientations called "microplanes". At each finite element integration point the microplanes can be imagined to represent damage or weak planes of the microstructure of the material. The macroscopic response is obtained by integrating contributions of all microplanes. More detail related to the used model can be found in Ožbolt et al. (2001).

The analysis was performed in the framework of continuum mechanics, i.e. smeared crack approach was used. In order to obtain results which are with good approximation independent from the element size, crack band approach (Bažant et. al. 1983) was used.

The bond between longitudinal reinforcement and concrete was simulated using discrete bond elements. For transverse reinforcement, a rigid connection between steel and concrete was assumed. This assumption neglects the influence of the relative displacement between stirrups and concrete. The discrete bond model implemented in MASA consists of a 1D nonlinear springs with a bond-slip relationship (see Fig. 6), which depends on the state of stresses and strains in concrete and reinforcement, on type of loading and geometry. More information related to the bond model can be found in Lettow (2006). It was demonstrated that the model is able to correctly predict bond behavior of deformed steel bars for monotonic and cyclic loading (Eligehausen et al. 1983, Lettow 2006). In Figure 6 the assumption for the bond-slip cyclic relationship for deformed bars is shown. Bond degradation is assumed to occur after a certain slip due to the mechanical damage of the concrete-steel interface produced by the ribs of the reinforcement bars. More detail can be found in Eligehausen et al. (1983).

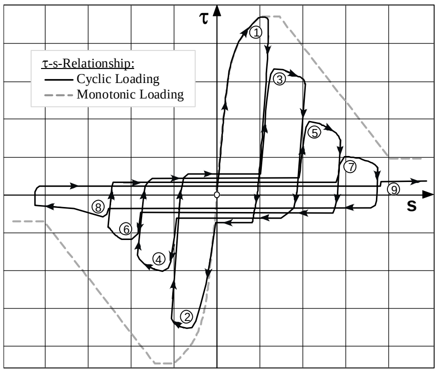

Figure 6. Bond-slip cyclic relationship for deformed bars (Eligehausen et al. 1983).

4.1 *Model discretization*

The concrete was simulated with hexahedral elements with side length of approximately 20 mm in the joint area and growing mesh size in those parts of the specimens which remained elastic. The boundary conditions were defined as nodal load and constraints. To the prevent the local failure of single concrete elements due to excessive stress distributions in the vicinity of the supports and at the zones of load application, the elements were taken as linear elastic (See darker elements in Fig. 7a).

Since the 1D reinforcement elements implemented in the MASA have no bending stiffness, extra stiffness had to be defined in the beam bars anchorage are, in order to properly simulated the forces transfer from the beam bars into the diagonal strut in the joint core.

In the analyses, the vertical symmetry of the specimen was utilized, i.e. only one-half of the beam-column connection was modeled. This allowed a high reduction of the computational time reducing the amount of nodes and element to 23,080 and 19,492, respectively.

The material properties of concrete and reinforcement adopted in the analysis were chosen according to Table 1 and the bond stress-slip relationships for the longitudinal reinforcement according to the values proposed by Lettow (2006).

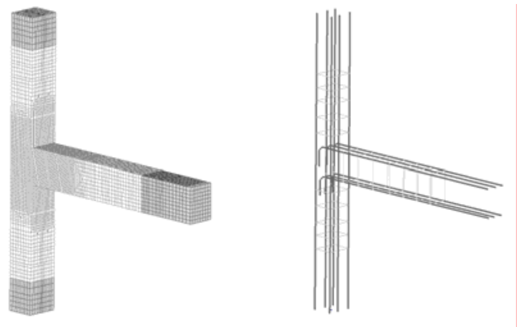

a) b)

Figure 7. FE Model (JT4-1): a) Discretization of concrete; b) Discretization of reinforcement.

5 NUMERICAL ANALYSES

After the calibration of the numerical model presented in Section 5.1, an extensive parametric study was performed. The main results are presented in Sections 5.2 and 5.3. In the following sections only the specimen JT4-1 is taken into account.

5.1 *Model calibration*

In this Section the results of the simulation of the test JT4-1 are presented. This test was chosen as benchmark for the numerical study to investigate the effect of different anchorages. For the calibration of the numerical model the greatest emphasis was given to the representation of the failure mode in terms of correct simulation of the cracking pattern according to the following sequence of events:

I. Cracking at beam-joint interface;
II. Cracking at column-joint interface;
III. Formation of 1st shear crack in positive loading direction (beam bar bent away from the joint);
IV. Formation of 1st shear crack in negative loading direction (beam bar bent into the joint);

V. Reach of peak load with a ratio of 1.5 between the two directions;
VI. Stiffness and strength degradation, either for consecutive cycles at the same displacement level, as well as at increasing displacement levels beyond 2% drift and high pinching.

The initial stiffness up to the first shear crack was overestimated in the numerical simulations (Fig. 8), but the core deformation was simulated with an acceptable confidence (Fig. 9). The correspondence of the post-peak behavior was better in the positive than in the negative direction. As shown in Figure 9 the experimental, as well as the numerical results confirm the assessment method proposed by Priestley (1997) and Pampanin et al. (2002). The joint has an almost negligible deformation up to the formation of the first shear crack, when the shear distortion starts increasing. In Table 2 the main results of experimental and numerical tests are summarized.

The correspondence of the cracking pattern of the experimental test and the numerical simulation is shown in Figure 10. It can be observed that the crack starting from the bottom hook (bent away from the core) is much flatter than the one starting from the top hook (bent into the core), as also observed in the experimental test. In the experimental tests, as well as in the numerical simulation for both the anchorage detailing the joint remained elastic up to a shear distortion. γ was approximately equal to 0.003 and 0.001 rad at the first shear crack and 0.008 and 0.014 rad at peak load for bars bent in and bent away, respectively. After the peak load high strength degradation was observed. Compared to the proposed joint shear strength-distortion curves (Fig. 1a), the shear strength had in both experimental and numerical test a higher degradation. The reason of the difference in the shear capacity, may be due to the effect of aspect ratio (h_b / h_c = height of beam / height of column), which is not considered in the assessment model, but it has a relevant influence as shown later in Section 5.3. For the configuration with bars bent away from the joint no proposal for the joint deformability was formulated yet.

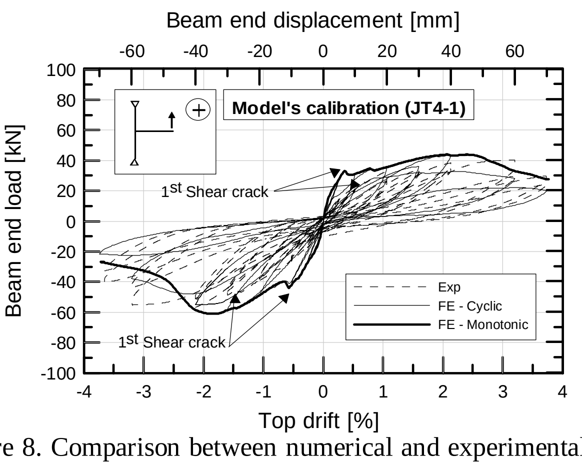

Figure 8. Comparison between numerical and experimental results: Hysteretic behavior of specimen JT4-1.

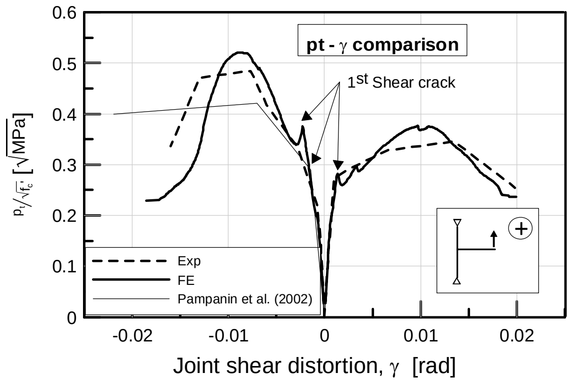

Figure 9. Comparison between numerical and experimental results: Joint deformation.

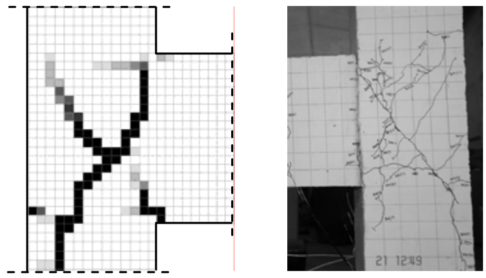

a) b)

Figure 10. Comparison of cracking of the joint panel in specimen JT4-1 at approx. 30 mm displacement: a) Numerical simulation; b) Experimental test.

Table 2. Comparison between experimental and numerical results.

Event		Exp	FE	FE/Exp
Initial stiffness [kN/m]	+	2980	5580	1.87
	-	3500	5530	1.58
First shear crack [kN] / [rad]	+	26.11	32.63	1.25
		0.0008	0.001	1.25
	-	46.60	41.15	0.88
		0.0030	0.0023	0.77
Peak load [kN] / [rad]	+	40.49	43.48	1.07
		0.0135	0.0110	0.81
	-	56.75	58.72	1.03
		0.0077	0.0086	1.11
Load at 1st cycle 70 mm [kN] / [rad]	+	29.86	20.17	0.70
		0.0198	0.0200	1.01
	-	39.35	21.49	0.55
		0.0160	0.0186	1.16

5.2 *Analysis of the failure mechanism*

In the calculation of the joint shear stress presented in this section, as well as in the parametric study in Section 5.3, the calculation of the internal lever arm of the beam in order to evaluate the shear force in joint panel, was assumed equal to 0.9*d*, with *d* static height of the beam, according to the method explained in Hakuto et al. (2000). This assumption is based on the results of the moment-curvature analysis of the beam. According to this calculation the ratio of shear capacity between the anchorages configurations with bars bent in and away from the joint is approximately 1.5.

From the strain gauges readings in the specimens and from the stresses in the tensioned beam bars in the FE simulations is possible to calculate the real internal lever arm of the beam section. The assumed lever arm of 0.9*d* is confirmed for the specific case of anchorage of bars bent into the joint, but it overestimates the value for the case of bars bent away from the joint, where a value of 0.75*d* at peak load seems to be more appropriate. These measurements seem to be confirmed comparing the compression stress fields in Figure 11c, d, where in the first case (bars bent away from the core) the compression zone in the beam is much higher. Taking this value into account, the difference of shear capacity between the considered anchorage configurations would decrease to approx.1.2 ÷ 1.3. However, for reason of simplicity, the lever arm calculated in the moment curvature analysis (0.9*d*) will still be assumed in this work.

Generally, according to the numerical simulations, the first shear crack in the joint core occurs when the concrete tensile stress in the tie is reached and the peak load corresponds with the failure of the compression strut (see Fig. 11). The more effective anchorage of beam bars bent into the joint core can be seen comparing Figure 11a, b, where at the formation of the first shear crack, the tensile stress in the core is more distributed in Figure 11b and Figure 11a. Comparing Figure 11c, d it can be observed that the concrete strut is much steeper in the case of beam bars bent into the joint, but it has also a much bigger width. This explains the different joint shear capacity for the two anchorage configurations.

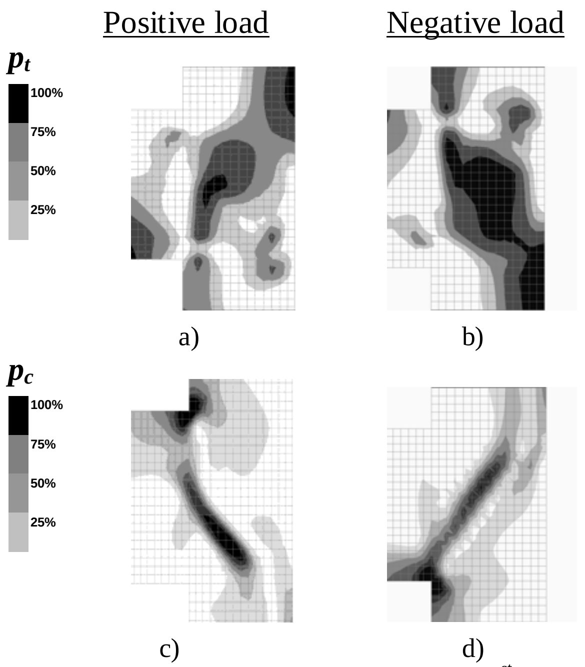

Figure 11. a), b) Tensile stresses in the core at 1st shear crack; c), d) Compressive stresses in the core at peak load.

5.3 *Parametric study*

The influence of several parameters on the first shear crack formation and on the peak load was investigated and in this section the main results are presented.

The variation of the concrete strength (Fig. 12) confirms the validity of the adopted model presented in Section 2, since the calculated *k*-factor is with acceptable approximation invariant with respect to the concrete strength. An increase of beam reinforcement ratio (Fig. 13) seems to induce an increase of the peak load. This may be explained with a higher tensional demand in the hook, if the portion of the tension force in the beam bars transferred in the concrete by bond is less (lower reinforcement ratio). This fact is more evident in the negative direction, (bar bent into the joint), since the hook bent away from the core is less effective in the formation of the concrete strut (Hakuto et al. 2000). The formation of the first shear crack in the joint seems to be less influenced by the amount of beam reinforcement. Similar results were obtained in numerical simulations by Hegger et al. (2004). The influence of column reinforcement ratio can be neglected with good approximation as shown in (Fig. 14). The formation of the first shear crack in the core seems to be slightly influenced. None of the investigated parameters seems to influence the joint deformability (first crack and peak load). Only increasing the concrete strength, at peak load the joint shear distortion decreases.

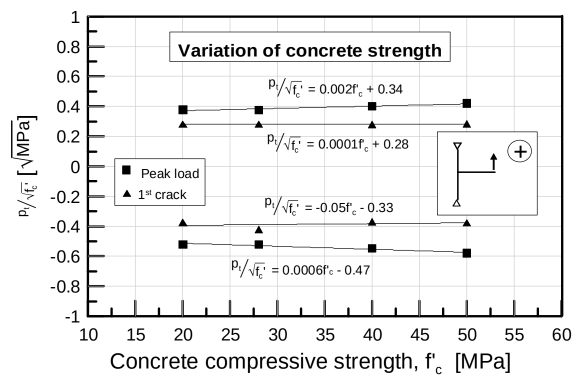

Figure 12. Effect of variation of concrete strength on the joint shear capacity.

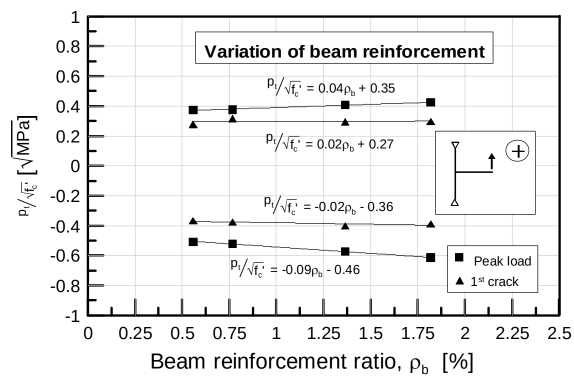

Figure 13. Effect of variation of beam reinforcement on the joint shear capacity.

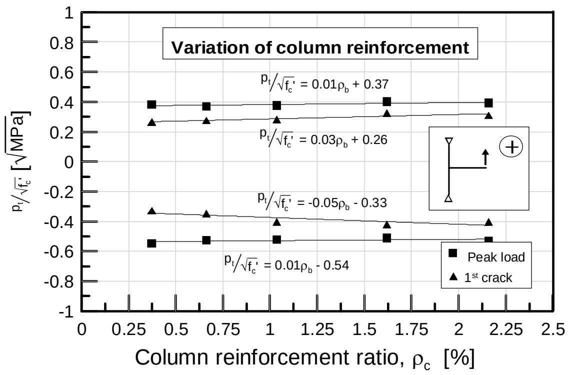

Figure 14. Effects of variation of column reinforcement on the joint shear capacity.

Even if the influence of the joint aspect ratio is not accounted for by the model proposed by Priestley (1997), it was recognized by other authors that it has a very high influence on the shear capacity of the joint (e.g. Hegger et al. 2003, Vollum & Newman 1999). In Figure 15 the influence of this parameter according to the numerical simulation as well to the proposals by Hegger and Vollum is shown for the case of bars bent into the joint. The compared models show similar trends. The influence of the aspect ratio is due to the change of inclination of the compression strut, which becomes steeper with increasing h_b / h_c with consequent increase in the demand in order to balance the horizontal shear in the core. For bars bent away from the joint, the numerical simulations indicated an almost negligible influence of the aspect ratio, but more research work is needed to validate this statement.

The variation of axial load was not considered in this study, but it was already shown that this parameter is well taken into account by Priestley (1997), at least until the diagonal tension cracking initiates, since the principal tension stress instead of the shear stress is limited.

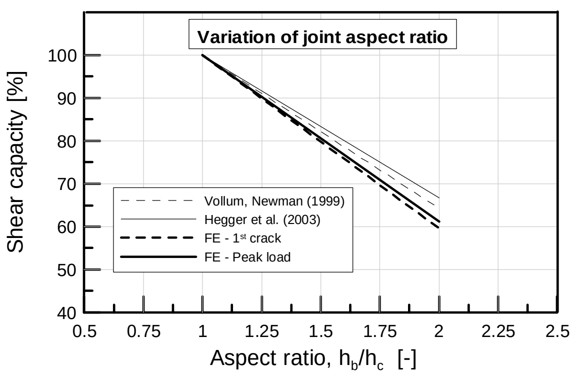

Figure 15. Variation of aspect ratio (h_b / h_c) for the case of bars bent into the joint.

Further analyses were performed in order to investigate the change of failure mode between joint shear and beam flexure (Fig. 16). It was observed that, if the beam yielded before the formation of the first crack, a ductile failure occurred (Beam 1 and 2). When, instead, the beam yielding occurred after the formation of the first crack, the flexural mechanism was not stable and a brittle mechanism through joint shear cracking was not avoided. The capacity of the connection in this case was even lower of the one of the benchmark test, where the beam reinforcement did not yield (compare “Shear” with “Beam / Shear”).

Furthermore, it is interesting to observe that in the failure “Beam 2” a shear cracking in the joint core occurred just before the target displacement of 70 mm was reached, which can also be seen from the step in the load-displacement curve (see Fig. 16).

Observing Figure 17 the role of the formation of the first shear crack is evident. Only in the simulation “Beam 1” the joint core did not reach the distortion of 0.002 rad, which corresponds to the cracking of the joint and in that case the core remained intact during the whole analysis.

A degradation curve of the joint shear stress resisted by concrete as function of the curvature ductility factor valid for exterior joints has been proposed by Park (1997), but the influence of beam flexural yielding on the joint shear capacity, seems to be much lower, than in the numerical investigations performed in this study.

Further research work is needed to define clear conditions to distinguish between beam flexural and joint shear mechanisms.

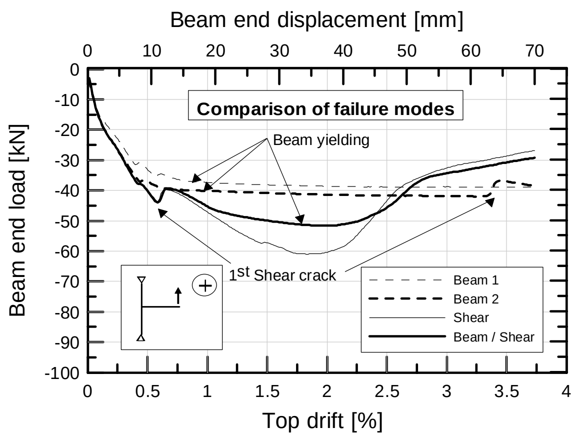

Figure 16. Interaction between beam flexural failure and joint shear cracking (load displacement curves).

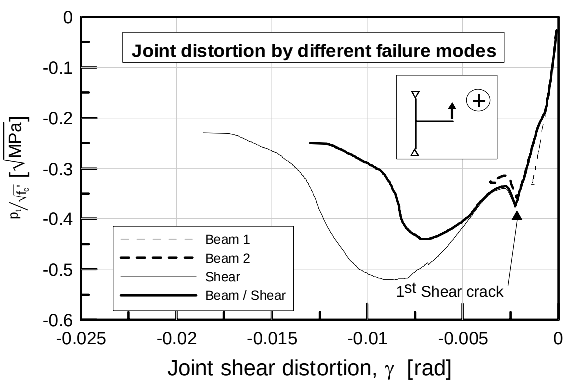

Figure 17. Interaction between beam flexural failure and joint shear cracking.($p_t - \gamma$ curves)

6 SUMMARY AND CONCLUSIONS

In the present paper the experimental work performed in order to evaluate the joint shear capacity of beam-column connections designed according to pre 1970s codes was briefly presented.

One of the performed tests was chosen for a numerical study by means of 3D non linear analysis using FE Code MASA based on a microplane model for concrete. The model calibration showed the capability to reproduce the hysteretic behavior and the joint shear distortion of the beam-column joint with acceptable confidence. Furthermore, the failure mode and relative cracking pattern could be realistically reproduced. Comparing Figure 9a, b it seems that the shear distortion vs. shear capacity can describe more accurately the seismic performance of the joint core, since in the hysteretic behavior in influences by beam, column and boundary conditions. The obtained results are well comparable with the proposal in Figure 1.

As already shown by Priestley (1997) and by other researchers (Pampanin et al. 2002) the initiation of first shear cracking in the joint is a fundamental event. From this event the joint contribution to the global deformation of the subassemblies starts increasing dramatically with consequent decrease of strength and stiffness of the specimen. For this reason in this study particular emphasis was given to the formation of the first diagonal crack.

The performed numerical analyses gave the possibility to visualize the principle tension and compression stresses and strain in the joint, which represent a fundamental instrument to improve the understanding of the complex mechanism that governs the behavior of the joint core.

A parametric study was carried out in order to evaluate the influence on the joint shear capacity of several parameters such as concrete strength, amount of beam and column reinforcement and joint aspect ratio. As already observed by other researchers in past, the joint aspect ratio (h_b / h_c) is the parameter which most influences the joint shear capacity and for this reason the authors of this paper believe in the importance to include it in joint assessment models based on p_t-γ strength degradation curves.

Further investigations are needed to assess the influence of the axial load on the failure of the concrete strut after the formation of the first crack.

The varied parameters did not influence significantly the joint deformability. If this statement will be confirmed in the future work, it could open the way for a simple definition of shear deformability limits, as invariant characteristics of the joint panel, as already proposed in FEMA 356.

The results of the numerical investigations have to be validated with a larger experimental database in order to better propose a safe and economical assessment method for the shear capacity of exterior beam-column joints designed according to old non-seismic codes.

REFERENCES

ACI Committee 318, 1971. Building Code Requirements for Structural Concrete (ACI 318-71), *American Concrete Institute*, Detroit, Mi, USA.

ACI Committee 318, 1995. Building Code Requirements for Structural Concrete (ACI 318-95), *American Concrete Institute*, Farmington Hills, Mi, USA.

Bažant, Z. P.; Oh B. H. 1983. Crack band theory for fracture of concrete. *Mater Struct RILEM;* 93 (16): 155-77.

Eligehausen, R.; Popov, E. P.; Bertero V.V. 1983. Local bond-stress relationships of deformed bars under generalized excitation, *UCB/EERC 83,23.*

Eurocode 8, Design Provisions for Earthquake Resistance of Structures, *European Committee for Standardization*, 1994, Brussels, Belgium.

FEMA 356, 2003. Prestandard and Commentary for Seismic rehabilitation of buildings. *American Society of Civil Engineers (ASCE).* Reston, VA, USA.

Hakuto, S.; Park, R.; Tanaka, H. 2000. Seismic Load Tests on Interior and Exterior Beam-Column Joints with Substandard Reinforcing Details. *ACI Struct J.* 97(1): 11-25.

Hegger, J; Sherif, A.; Roeser, W. 2003. Non Seismic Design of Beam Column Joints. *ACI Struct J* 100(5): 654-664.

Hegger, J; Sherif, A.; Roeser, W. 2004. Nonlinear finite element analysis of reinforced concrete beam-column connections. *ACI Struct J* 101(5): 604-614.

Hertanto, E. 2006. Seismic Assessment of pre 1970s reinforced concrete structure. *MS Thesis, University of Canterbury*, Christchurch, NZ.

Kurose, Y. 1987. Recent Studies on Reinforced Beam-Column Joints in Japan. PMFSEL Report No. 87-4, University of Texas at Austin, USA.

Lettow, S. (2006) Ein Verbundelement für nichtlineare Finite Elemente Analysen – Anwendung auf Übergreifungsstöße, *PhD Dissertation, IWB, University of Stuttgart*, Germany (in German).

NZS 3101:1995. Design of Concrete Structures – Vols. 1 and 2. *Standard Association of New Zealand*, Wellington, NZ.

Ožbolt, J.; Li, Y; Kožar 2001. Microplane Model for Concrete with Relaxed Kinematic Constraint. *International Journal of Solid and Structures.* 38: pp. 2683-2711.

Pampanin, S.; Calvi G. M.; Moratti, M. 2002. Seismic Behaviour of RC Beam-Column Joints Designed for Gravity Loads (Paper 726). *12th European Conference on Earthquake Engineering*, London, UK.

Pampanin. S., 2006 Controversial Aspects in Seismic Assessment and Retrofit of Structures in Modern Times: Understanding and Implementing Lessons from Ancient Heritage *NZSEE Bulletin*, 39(2): 120-133.

Park, R. 1997. A static force-based procedure for the seismic assessment of existing reinforced concrete moment resisting frames. *Bulletin of the New Zealand National Society for Earthquake engineering.* 30(3): 213-226.

Priestley, M. J. N. 1997. Displacement-Based Seismic Assessment of Reinforced Concrete Buildings. *Journal of Earthquake Engineering* 1(1): 157-192.

Vollum, R.; Newman, J. 1999. The design of external reinforced concrete beam-column joints. *The Structural Engineer*, Band 77.